PHYSICAL REVIEW E **73**, 065301(R) (2006)

Foaming dynamics in Hele-Shaw cells

H. Caps* and N. Vandewalle
GRASP, Institut de Physique B5, University of Liège, B-4000 Liège, Belgium

G. Broze
Colgate-Palmolive, Zoning industriel des Hauts-Sarts, B-4000 Liège, Belgium

(Received 14 December 2005; published 1 June 2006)

We have studied foaming dynamics in Hele-Shaw cells partially filled with a soap and water mixture. A series of upside-down flips produces an intermittent wetting of the cell and leads to foam formation. As a function of the number of flips, an increasing number of bubbles composes the foam, until saturation is observed. Statistical analysis shows that the bubble size follows a Gamma distribution. Contrary to common belief, this foaming dynamics by "shaking" creates homogeneous foam, even though the system may pass through transient heterogeneous configurations. A mechanistic interpretation is proposed and included into a theoretical model.

DOI: 10.1103/PhysRevE.73.065301 PACS number(s): 47.55.db, 47.55.df, 82.70.Rr, 83.80.Iz

Foams are widely used in common life applications, ranging from dishwashing liquids to acoustic isolation. Aqueous foams are characterized by a liquid fraction, defined as the volume of liquid relative to the volume of gas. Dry foams (liquid fraction of a few percent) are composed of polyhedral bubbles separated by thin films meeting at the Plateau borders [1], while wet foams (liquid fraction $\phi \sim 30\%$) are composed of spherical bubbles [2]. On Earth, dry and wet foams coexist. Gravitational downward motion of the liquid through Plateau's borders dries the top of the foam while the bottom remains wet thanks to capillarity. Numerous works have addressed foam drainage, both experimentally [3–7] and within the drainage equation formalism [8,9]. Analytical solutions are now available for modeling foam drainage in various experimental conditions [9]. On the contrary, only a few papers [10] report on foam generation techniques (shaking, air blowing, and so on) and the resulting bubble size distributions.

The present Rapid communication reports on foam generation by successively flipping a container partially filled with a surfactant and water mixture. Due to wetting on the container walls, thin liquid films are created during each flip. Starting with a large bubble over a liquid pool, we show that successive flips lead to the generation of a foam composed of many bubbles. This foam obeys statistical laws that are highly reproducible.

The experimental setup consists of a Hele-Shaw (HS) cell ($13 \times 13 \times 0.3$ cm^3) partially filled with a sodium dodecyl sulfate–water mixture [ten times above the critical micellar concentration (cmc)]. The amount of liquid, relative to the cell volume, is denoted φ. The cell is fixed from the top to a horizontal rod set into rotation with the help of a motor managed by a microcontroller. The cell is then flipped upside down within one second such that inertial forces dominate and cause the liquid to be drained toward the bottom of the cell. Wetting on the HS walls creates new bubbles [11]. Larger bubbles might also be split by falling droplets.

After each flip, the cell is left at rest for a while to be drained. The time needed for reaching the foam steady state depends on the surfactant [12] and is typically 10 s in the present case. A picture of the cell is taken after each flip and an algorithm has been developed to count the number of bubbles on the images, to measure their sizes, positions, and shapes. Figure 1 shows typical images of the foam at six different stages.

During the flips, the number N of bubbles increases (see Fig. 2) and is observed to tend to an asymptotic value N_∞, which depends on the initial liquid content φ. Within the range $0.02 < \varphi < 0.25$, the asymptotic number of bubbles increases with φ. On the contrary, for larger φ values, N_∞ decreases. This is due to the smaller volume of gas available for creating bubbles. The highly reproducible value of N_∞ in the experiments has to be emphasized.

First, the maximum number of bubbles that can be created depends on the amount of liquid present in the cell. For smaller φ values, all the liquid is rapidly stacked in the Plateau borders and bubble edges. In such a case, conservation of mass leads to

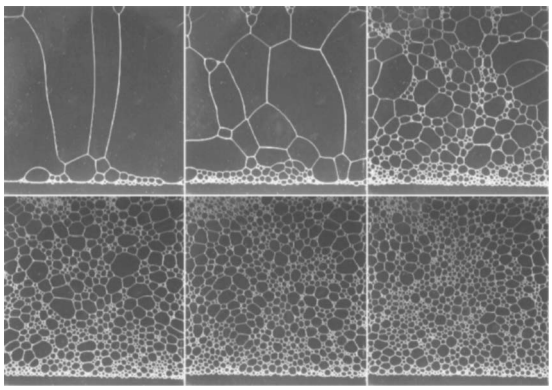

FIG. 1. Six consecutive images of the foam in the HS cell after $n_f = 1, 2, 6, 12, 18, 24$ flips. Images cover the 13×13 cm^2 area of the HS cell.

*Electronic address: herve.caps@ulg.ac.be

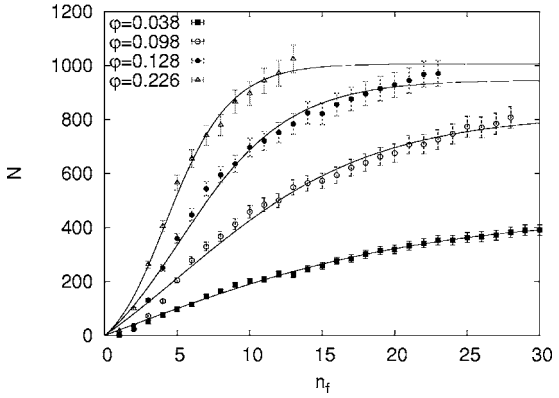

FIG. 2. Number N of bubbles as a function of the number n_f of successive flips. Different liquid content values φ are illustrated. Solid curves are fits using our model [see Eq. (7)].

$$N_\infty \sim \frac{A(1-\varphi)}{\varepsilon \ell}, \tag{1}$$

where A is the HS area, ℓ is the characteristic length of the bubbles, and ε is a length related to the width of the Plateau borders. Later, we show that a low φ value is not the only source of limitation for N_∞.

The series of flips leads to an evolution of the statistical distribution of the bubble sizes s, defined as the area covered by the bubbles on the images. Typical experimental cumulative distributions are given in Fig. 3. χ^2 tests [13] revealed that the foam exhibits a Γ distribution $f(s)$, given by

$$f(s) = \frac{1}{\beta^\alpha \Gamma(\alpha)} s^{\alpha-1} \exp\left(\frac{-s}{\beta}\right), \tag{2}$$

where Γ is the Γ function. Statistical estimators for parameters shape α and scale β are obtained from experimental results:

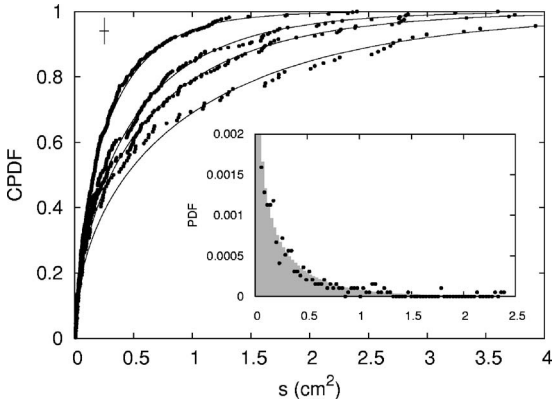

FIG. 3. Cumulative probability distribution (CPDF) of the bubble sizes s. Distributions are given at four different stages n_f=6,10,14,29 flips for a liquid content φ=0.038. The inset shows a typical PDF (n_f=10 flips) where the gray histogram is a Γ distribution based on the estimators Eq. (3). The cross at top left gives typical error bars for all data points.

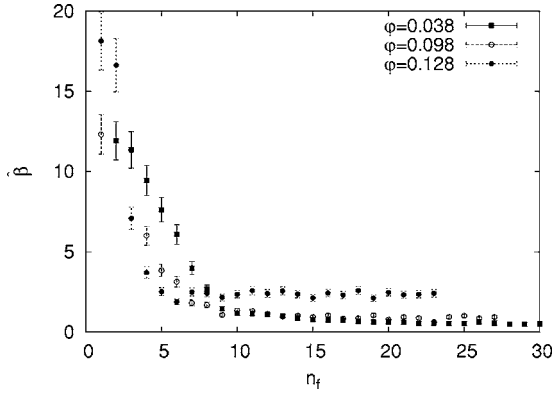

FIG. 4. Ratio between the standard deviation of the bubble size distribution $\sqrt{\sigma_s}/\bar{s}$ and the mean bubble size $\bar{s}$ as a function of n_f. Different liquid contents φ are illustrated.

$$\hat{\alpha} = \left(\frac{\bar{s}}{\sqrt{\sigma_s}}\right)^2 \quad \text{and} \quad \hat{\beta} = \frac{\sigma_s}{\bar{s}}, \tag{3}$$

where σ_s is the variance of the data set and $\bar{s}$ is the mean bubble size. Both parameters evolve during the foam formation and are functions of the liquid content value. Typical values of the parameter $\hat{\alpha}$ range from 0.1 ± 0.01 to 0.5 ± 0.05 and are larger for large φ values since σ_s decreases faster when more liquid is used. Characterization of foam homogeneity is better revealed by $\hat{\beta}$ and is discussed below.

While a Poisson distribution describes a waiting time until the occurrence of a probable event, a Γ distribution holds for the waiting times until α Poissonian events occur. Herein, the waiting time should be associated with the bubble fragmentation process [14]. As a function of n_f, the parameter β is observed to decrease by one order of magnitude (see Fig. 4). The asymptotic value gives a minimum bubble size that cannot be over-passed. The continuous curves in Fig. 3 are the predicted theoretical probability distributions based on experimental data, represented by the black dots. The agreement between theoretical distributions and experimental data is remarkable, and passed χ^2 tests. If least-squares fit to the data are performed with Γ distributions, the fit parameters differ from estimated ones [Eq. (3)] by only a few percent. However, for small n_f values, the small number of bubbles leads to noisy statistics and less agreement—errors on estimated parameters can reach 25%. It should be noted that such space occupation obeying a Γ distribution was also observed in previous theoretical and numerical studies on Voronoi tesselation in two [16] and three dimensions [17]. These studies [16] showed that geometrical constraints, such as the angle between adjacent soap films, may play a role in these statistical distributions. Such conclusions could be experimentally tested in the present setup.

A remarkable feature of the system is the fast decrease of the standard deviation of the bubble size distribution during the successive flips. This decrease may reveal a homogenization of the bubble sizes but may also be due to the growth of N. More precisely, the foam homogeneity is not represented by the standard deviation but rather by the ratio of that standard deviation $\sqrt{\sigma_s}$ to the mean bubble size $\bar{s}$. Figure

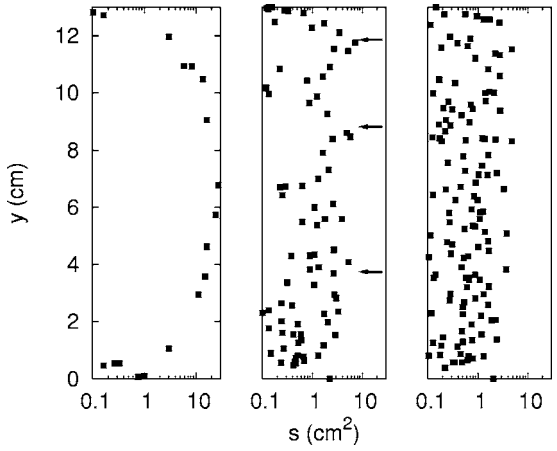

FIG. 5. Semilogarithmic plot of the mean bubble size $\bar{s}$ found at a given height y. From left to right, pictures correspond to $n_f=2,6,10$ flips for a liquid content $\varphi=0.038$. Arrows in the middle picture indicate clusters of large bubbles.

4 shows the evolution of that ratio during the successive flips, for different values of φ. This figure emphasizes that the mean bubble size is getting smaller during foaming. More important, the foam is generated in such a way that it becomes monodisperse.

In addition to bubble size distribution, a foam is characterized by its spatial homogeneity. This latter is related to the foam stability since avalanches [15] and gas diffusion [1] depend on the way the bubbles are organized. Figure 5 presents the mean bubble size of the bubbles found at a given height of the HS cell after different flip numbers. As the experiment commences (left panel), most of the small bubbles are located near the top and the bottom of the cell while large bubbles are seen around the center. This size segregation is mainly due to small bubbles that can either be trapped by the falling fluid flow or be pushed up during the foam drainage. As the foam is generated, clusters of large bubbles are found in different places in the cell. In the middle picture of Fig. 5, these regions are denoted by small arrows. Eventually, these large bubbles are broken and the foam becomes homogeneous, as emphasized in the right panel of Fig. 5.

The bubble breakup process has been studied with the help of a high-speed video camera. On Fig. 6, a typical series of six successive images during a bubble split process is presented. This sequence has been recorded at a frame rate of 100 frames/s from the moment the cell was in the vertical position. The falling fluid creates small droplets, which may carry small bubbles. This descending motion is clearly seen to cause the bubble split. For clarity reasons, the breaking bubble has been drawn in light gray. From this observation, it appears that transport of small bubbles into the fluid flow is responsible for the primary bubble segregation observed after a few flips (see Fig. 5).

After a large number of flips, no more breakup is observed. This stationary state is related to the minimum bubble size. For small liquid content (not illustrated), this asymptotic bubble size is quite large because most of the fluid is retained in the foam. For larger φ values, all experiments present the same limit. The impossibility of breaking bubbles smaller than a given size can be explained in terms of the capillary length

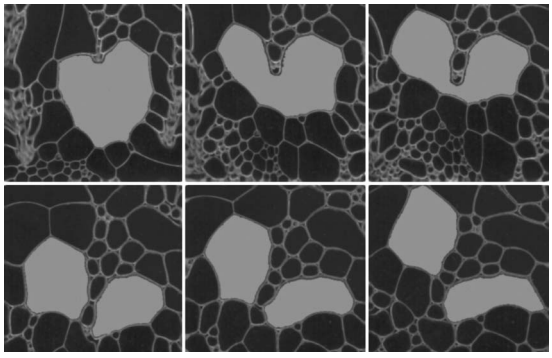

FIG. 6. Typical split sequence recorded at a frame rate of 100 frames/s. A large bubble (colored in light gray) is observed to be broken by the falling liquid.

$$\ell_c = \sqrt{\frac{\gamma}{\rho g}}, \tag{4}$$

where γ is the surface tension of the liquid, ρ is its density, and g is the Earth gravitational acceleration. In Fig. 7, we have plotted the square root of the mean bubble size $\bar{s}$ divided by the capillary length. It is then found that all curves tend to the ratio

$$\frac{\sqrt{\bar{s}}}{\ell_c} \approx 1.6. \tag{5}$$

This behavior suggests that the system tends to a state characterized by bubbles having a characteristic length that is 1.6 times the capillary length. This value for the ratio between the square-root of the area and the characteristic length corresponds to regular hexagons with sides of length ℓ_c. This result evidences the fact that the successive flips lead to a homogeneous foam composed of nearly hexagonal bubbles. This is in agreement with Plateau's rules [1].

For bubbles smaller than the capillary length, falling droplets simply slip on the bubble edges and no breakup occurs. Experimental bubble size distributions reveal that above this minimal length, all bubbles are equivalently able to split; a Γ distribution is indeed observed. The number of

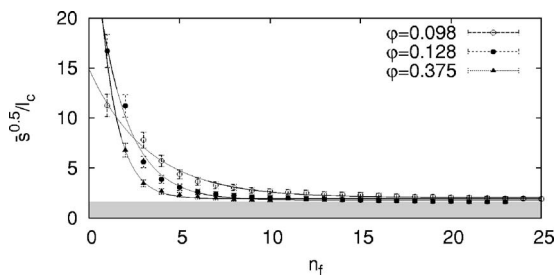

FIG. 7. Square root of the mean bubble size $\bar{s}$ divided by the capillary length ℓ_c as a function of number of flips. Different values of the liquid content are illustrated. The gray region corresponds to values below 1.6.

bubbles that can be split also depends on the amount of available liquid. This amount decreases as the number of bubbles increases. Considering these arguments, the temporal evolution of the number of bubbles may be driven by the kinematic equation

$$\frac{dN}{dn_f} = aN\left(\varphi - N\frac{\varepsilon\ell}{A}\right). \tag{6}$$

The product $\varepsilon\ell$ corresponds to the amount of liquid surrounding each bubble. As time goes on, ℓ is expected to tend toward the capillary length. Meanwhile, $\ell = \sqrt{A/\xi N}$, where ξ depends on the ratio between the bubble area s and its characteristic length ℓ (1.6 here). Injecting this last relationship into the evolution equation, one gets a differential equation admitting the solution

$$N = \varphi^2 \frac{\exp(a\varphi n_f)}{\left(1 + \frac{\varepsilon}{\sqrt{\xi A}}\exp\left(\frac{a\varphi n_f}{2}\right)\right)^2}. \tag{7}$$

The initial condition for fitting this solution to experimental data $[N(0)=1]$ reduces the number of unknown variables. The fit parameter a corresponds to the bubble split rate and should be related to fluid and surfactant properties. At low liquid fraction $a \approx 0.004$, while it is estimated as 0.07 ± 0.02 for $\varphi = 0.38$. Fits to the data using this law are presented in Fig. 2. A good agreement between experiment and theory is noted. Errors on fitting parameters are roughly 20%, which is acceptable, in view of the small number of experimental data points accessible near saturation. This theoretical model shows that the maximum number of bubbles that can be created directly depends on the liquid content φ. As previously stated, the growth of N_∞ with φ is, however, limited to values of the liquid content smaller than 0.25. From similarity with Voronoi constructions, one way to grasp the experimental behavior at all φ values might be to include a geometrical description of the HS cell.

In summary, we proposed an elegant method for producing two-dimensional foams in a highly reproducible way. With a series of successive flips of a HS cell, a foam is produced and exhibits a Γ distribution for the bubble size distribution. The mean bubble size of this distribution tends to an asymptotic value that is related to the capillary length. The foam is also spatially homogeneous. This method could thus be applicable to foaming characterization and, moreover, shows that reproducible foams can be produced by shaking. In the future, this system could also be extended to foam decay studies.

H.C. benefits from a grant from FNRS (Brussels, Belgium). We thank D. Weaire, S. Cox, and S. Dorbolo for fruitful discussions. This work is financially supported by ESA (MAP Grant No. AO-99-108) and Colgate-Palmolive.

[1] J. Plateau, *Statique Expérimentale et Théorique des Liquides Soumis aux Seules Forces Moléculaires* (Gauthier-Villars, Paris, 1873).
[2] D. Weaire and S. Hutzler, *The Physics of Foams* (Clarendon Press, Oxford, 1999).
[3] H. Caps, H. Decauwer, M.-L. Chevalier, G. Soyez, M. Ausloos, and N. Vandewalle, Eur. Phys. J. B **33**, 115 (2003).
[4] S. A. Koehler, S. Hilgenfeldt, and H. A. Stone, Langmuir **16**, 6327 (2000).
[5] M. U. Vera and D. J. Durian, Phys. Rev. Lett. **88**, 088304 (2002).
[6] S. A. Koehler, H. A. Stone, M. P. Brenner, and J. Eggers, Phys. Rev. E **58**, 2097 (1998).
[7] M. Durand, G. Martinoty, and D. Langevin, Phys. Rev. E **60**, R6307 (1999).
[8] G. Verbist, D. Weaire, and A. M. Kraynik, J. Phys.: Condens. Matter **8**, 3715 (1996).
[9] S. J. Cox and G. Verbist, Microgravity Sci. Technol. **14**, 45 (2003).
[10] R. J. Pugh, Adv. Colloid Interface Sci. **64**, 67 (1996).
[11] W. Drenckhan, S. Gatz, and D. Weaire, Phys. Fluids **16**, 3115 (2004).
[12] M. Duranda and D. Langevin, Eur. Phys. J. E **7**, 35 (2002).
[13] K. Bury, *Statistical Distributions in Engineering* (Cambridge University Press, Cambridge, U.K., 1999).
[14] S. Bohn, L. Pauchard, and Y. Couder, Phys. Rev. E **71**, 046214 (2005).
[15] N. Vandewalle, J. F. Lentz, S. Dorbolo, and F. Brisbois, Phys. Rev. Lett. **86**, 179 (2001).
[16] S. Kumar, S. K. Kurtz, and D. Weaire, Philos. Mag. B **69**, 431 (1994).
[17] E. Pineda, P. Bruna, and D. Crespo, Phys. Rev. E **70**, 066119 (2004).